

TABLE I. Energy dependence of nuclear events.

Energy (in Mev)	Σl (in cm)	Stars	Stops	Elast. scatt. ($>30^\circ$)	Inelast. scatt.
30- 50	2145 ± 21	49 (15)	8	8 (17)	2 (6)
70- 80	1438 ± 14	44 (11)	4	4 (4)	7 (8)
60- 90	1000 ± 50	19 (7)	4	3 (6)	6 (8)
100-110	2761 ± 28	76 (16)	18	15 (20)	22 (32)

measurements. It was possible to obtain plates covered by such a uniform and well-collimated flux that scanning "along the track" (with 90X, 80X, and 43X oil objectives) was as rapid as the conventional area scanning, and was employed exclusively in this work.

The actual numbers of the nuclear interactions observed in the total path of meson track followed, Σl , are given in Table I. In this classification we define "elastic scattering" as an event in which the incident and scattered pi-meson differ in energy by less than 15 percent. Occasionally, these may be accompanied by a short black prong or slow electron (10-100 kev) at the vertex. "Inelastic scatterings" are defined as events in which the scattered meson demonstrates, by grain density and plural scattering measurements, an energy loss >15 percent of the energy of the incident meson. When the outgoing track is shorter than 700 microns, only its grain density can be determined and the distinction between mesons and protons is not completely certain. The figures enclosed by brackets in columns 5 and 6 include these doubtful scatterings. In the third line, the data obtained in the old (60-90 Mev) meson beam¹ are also reported. The bracketed figures in column 3 give the number of stars having a proton prong of at least 30 Mev.

The angular distribution of the elastic scatterings $<30^\circ$ strongly suggests that most of these can be considered as shadow and coulomb scattering or $\pi-\mu$ -decays. Since the results are quite insensitive to the choice of this cut-off angle, we assume that the remaining events are true interactions of pi-mesons with the nuclear matter in the emulsion. Table II gives the total number Σn

TABLE II. Corrected mean free path.

Energy (Mev)	$I(e)$ (percent)	$I(\mu)$ (percent)	$\Sigma'(l)$ (cm)	Σn	λ_{geom} (cm)	λ_{obs} (cm)
30- 50	(3 \pm 2)	(8 \pm 4)	1910 ± 100	80	15.6	24.0 ± 3.0
70- 80	(10 \pm 2)	(9 \pm 3)	1165 ± 55	60	19.1	19.4 ± 2.6
60- 90*	(10 \pm 5)	(10 \pm 5)	800 ± 100	37	20.4	21.5 ± 4.2
100-110	2	(5 \pm 3)	2610 ± 100	146	20.4	18.0 ± 1.3

* Old meson beam.

of these and the corresponding total mean free paths. In the $I(e)$ and $I(\mu)$ columns, the relative fractions of the electrons and μ mesons of the different beams are given. These fractions were estimated principally by counter experiments.³ Further and consistent data were provided by cloud chamber runs⁴ and by analysis of track characteristics. The $\Sigma' l$ column gives the corrected path length of π^- meson observed. The geometrical mean free path, λ_{geom} , is taken to be

$$\lambda_{geom} = 1/\Sigma_i N_i \pi \hbar^2 [(A^1/\mu c) + (1/p)]^2,$$

where the summation is over the emulsion constituents. This includes the finite extent of the pi-meson wave packet. At high energy, $\lambda_{obs} \cong \lambda_{geom}$; at low energy there is a transparency of ~ 30 percent. Since probably less than 25 percent of the collisions involve the light elements, this transparency is believed to originate in an energy dependence of the character of the interactions. Table III gives the absolute cross sections in barns for the various types of interactions as a function of energy. In this table, the bracketed figures of Table I were employed. The stoppings are included with stars because of the information in the π^+ interactions (to be published), which strongly indicate that these are stars containing only neutron prongs.

TABLE III. Cross sections, in barns.*

Energy	Stars and stops	Elast. scatt. 30°	Inelast. scatt.	Total
30- 50	0.62	0.19	0.06	0.87
60- 90	0.76	0.10	0.19	1.05
100-110	0.75	0.16	0.25	1.16

* Obtained from $\sigma = (21/\lambda)$ barns.

The definite increase with energy of the relative frequency of catastrophic processes (absorption and inelastic scattering) with respect to the elastic scatterings can partially explain the discrepancy between the results, here presented, and those of Bradner and Rankin.⁵ However, in the energy interval (30-50 Mev) corresponding to the Berkeley experiment, the relative star frequency found by us is still twice that given by the Berkeley authors.

The general features of the stars do not change with the π^- energy, and it is evident that a large fraction of the absorbed energy is carried away by neutral particles (neutrons). However, a clearer analysis of the pion absorption mechanics will be possible through the comparison of these results with data now being assembled on the π^+ interactions.

We should like to acknowledge the invaluable assistance of Mr. Harrison Edwards, Mr. J. Spiro, and the Nevis staff, and to express appreciation to Mrs. N. Bernardini, Mrs. D. Lee, and Miss E. Wimmer for the scrupulous care taken in the scanning. Mrs. J. Bielk did excellent work in processing of the plates.

¹ Bernardini, Booth, Lederman, and Tinlot, Phys. Rev. **80**, 924 (1950).

² Bernardini, Booth, Lederman, and Tinlot, Phys. Rev. **82**, 105 (1951).

³ The authors wish to thank Professors A. Sachs and J. Steinberger, and Dr. P. Isaacs for informing them of their results. See also Chedester, Isaacs, Sachs, and Steinberger, Phys. Rev. **82**, 958 (1951).

⁴ Lederman, Booth, Byfield, and Kessler, **83**, 685 (1951).

⁵ H. Bradner and B. Rankin, Phys. Rev. **80**, 916 (1950).

Probable Emission of a Beryllium-8 Nucleus in the Fast Neutron Fission of Thorium-232

E. W. TITTERTON

Research School of Physical Sciences, Australian National University,
Canberra, Australia

(Received July 9, 1951)

IN the course of recent photographic plate experiments on the fast neutron fission of thorium-232 using 2.5-Mev D-D neutrons,¹ an event was observed in which two light particle tracks emanate from the point of fission in addition to the two heavy fragments. The event is very similar to that observed earlier by Goward, Titterton, and Wilkins² in the course of experiments on the photofission of uranium. The explanation suggested in the photofission case was that the event represented ternary fission with the emission of a Be⁸ nucleus. If the same explanation is applied to the present event, the α -particles are found to have energies of 10.0 and 9.6 Mev, respectively, and are inclined at 9° each other. Calculation shows that the energy release in the disintegration of such a Be⁸ nucleus into the two α -particles is 120 ± 10 kev. This is somewhat higher than the measured value for the instability of the ground state of Be⁸ given by Hemmendinger³ as 103 ± 10 kev, by Tollestrup, Fowler, and Lauritsen⁴ as 89 ± 5 kev, and more recently by Carlson⁵ as 72 ± 5 kev. Nevertheless, it seems reasonable to interpret the event as representing the fast neutron ternary fission of a thorium-232 nucleus, the third fragment being a Be⁸ nucleus in its ground state emitted with an energy of 19.6 ± 0.5 Mev at an angle of 62° to the fission fragment of smaller charge.

That such events are very rare is indicated by the fact that the two discussed above are the only ones observed in investigations including examination of 600,000 slow neutron events in-

duced in U^{235} , 12,000 fast neutron events in U^{238} , 14,000 fast neutron events in Th^{232} , 10,000 photofission events in U^{238} , and 2500 photofission events in Th^{232} .

This work was carried out while the author was still at A.E.R.E., Harwell, and thanks are due to the Director, Sir John Cockcroft, F.R.S., for permission to publish.

¹ E. W. Titterton, Phys. Rev. **83**, 673 (1951).

² Goward, Titterton, and Wilkins, Nature **164**, 661 (1949).

³ A. Hemmendinger, Phys. Rev. **75**, 1267 (1949).

⁴ Tollestrup, Fowler, and Lauritsen, Phys. Rev. **76**, 428 (1949).

⁵ R. R. Carlson, Phys. Rev. **83**, 203 (1951).

Inter-Ionic Distances and Line Widths in Paramagnetic Resonance Absorption

H. KUMAGAI, K. ŌNO, I. HAYASHI, H. ABE, J. SHIMADA, H. SHŌNO, AND H. IBAMOTO*

Institute of Science and Technology, Tokyo University, Tokyo, Japan

(Received July 3, 1951)

IN a previous letter,¹ we have reported some of the results of our precise observations on the line width in microwave paramagnetic resonance absorption by manganese sulfates, in conjunction with the theory of dipolar broadening by Van Vleck.² Since then, measurements on several salts containing copper ions were added to our data, which can be compared with theory more thoroughly than before.

Results are summarized in Table I. The widths in the table are

TABLE I. Paramagnetic absorption lines (9970 Mc).

Salts	Single crystal or powder	Shape of absorption line	Range of half-width by crystal orientation (Oersted)	Range of g -values
$Mn(NH_4)_2(SO_4)_2 \cdot 6H_2O$ (diluted)	single	several peaks not completely resolved	~ 70	—
$Mn(NH_4)_2(SO_4)_2 \cdot 6H_2O$	single	several peaks scarcely resolved	1000–2000	—
$MnSO_4 \cdot 5H_2O$	single	one peak, intermediate shape of gaussian and resonance curve	—	—
	powder	one peak, intermediate shape of gaussian and resonance curve	1250	2.06
$MnSO_4 \cdot 4H_2O$	single	one peak, intermediate shape of gaussian and resonance curve	980–1500	2.00–2.07
	powder	one peak, intermediate shape of gaussian and resonance curve	1140	2.04
$MnSO_4 \cdot H_2O$	powder	one peak, resonance curve	305	2.00
$MnSO_4$	powder	one peak, resonance curve	655	2.00
$Cu(NH_4)_2(SO_4)_2 \cdot 6H_2O$	single	two peaks, like gaussian curve	~ 230	2.0–2.3
$Cu(NH_4)_2Cl_4 \cdot 2H_2O$	single	one peak, resonance curve	90–230	2.05–2.20
$CuK_2Cl_4 \cdot 2H_2O$	single	one peak, resonance curve	110–250	2.05–2.20
$CuSO_4 \cdot 5H_2O$	single	one peak, resonance curve	50–220	2.04–2.24
	powder	—	300	—
$CuCl_2 \cdot 2H_2O$	single	one peak, resonance curve	55–70	2.03–2.23
$CuSO_4 \cdot H_2O$	powder	one peak, gaussian curve	310	2.19

obtained at half the maximum χ'' irrespective of the line shapes. As the g -values of salts containing Mn^{++} are almost isotropic, the half-width in polycrystals of $MnSO_4 \cdot H_2O$ and $MnSO_4$ have definite meanings. In the cases of $Cu(NH_4)_2(SO_4)_2 \cdot 6H_2O$ and diluted $Mn(NH_4)_2(SO_4)_2 \cdot 6H_2O$, the curves are composed of several peaks which can be decomposed to one, and the widths of each are shown in the table. As the line shapes of polycrystals of $CuSO_4 \cdot H_2O$ are almost gaussian, it is probable that g -values are nearly isotropic in the single crystal.

We shall consider the line widths for the same kind of paramagnetic ions contained in various salts which have different inter-ionic distances. According to Van Vleck's theory,³ the widths $(\Delta H)_i$ owing to dipolar coupling in this case are given approximately as follows:

$$(\Delta H)_i \sim 1/r^3,$$

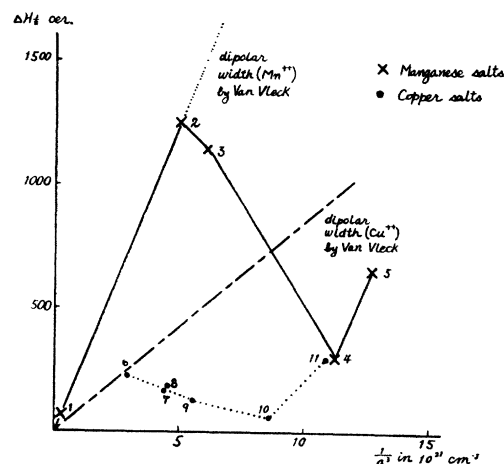


FIG. 1. Half-widths of salts of Mn^{++} and Cu^{++} and calculated dipolar widths. 1. $Mn(NH_4)_2(SO_4)_2 \cdot 6H_2O$ diluted; 2. $MnSO_4 \cdot 5H_2O$; 3. $MnSO_4 \cdot 4H_2O$; 4. $MnSO_4 \cdot H_2O$; 5. $MnSO_4$; 6. $Cu(NH_4)_2(SO_4)_2 \cdot 6H_2O$; 7. $Cu(NH_4)_2Cl_4 \cdot 2H_2O$; 8. $CuK_2Cl_4 \cdot 2H_2O$; 9. $CuSO_4 \cdot 5H_2O$; 10. $CuCl_2 \cdot 2H_2O$; 11. $CuSO_4 \cdot H_2O$.

where r is the mean inter-ionic distance, and the line shape is assumed to be gaussian. As a first approximation, we consider the arrangement of ions as simple cubic with lattice constant a ; then we can put $(\Delta H)_i \sim (1/a^3)$. The values of a are given by $a^3 \rho = M/N$ where ρ is the density, M the molecular weight related to the single ion of the salt, and N the Avogadro number.

In Fig. 1 the values of $(\Delta H)_i$ from Table I are plotted against $1/a^3$. The widths indicated in the figure for single crystals are means of those for different orientations. The dotted and dashed straight lines indicate the widths for Mn^{++} and Cu^{++} owing to dipolar broadening, by Van Vleck's calculation.² For smaller values of $1/a^3$, the widths are almost equal to those expected by dipolar broadening in both cases of Mn^{++} and Cu^{++} . But when ions are nearer, the width becomes much smaller than those corresponding to the straight lines, because of the effect of exchange interaction. These results agree with the fact that Δ , the departure from Curie's law in the static susceptibility, is 0.7° , 3° , 2° , and 24° for $Mn(NH_4)_2(SO_4)_2 \cdot 6H_2O$, $MnSO_4 \cdot 5H_2O$, $MnSO_4 \cdot 4H_2O$, and $MnSO_4$, respectively, and that Δ is mainly due to the exchange effect for manganese salts.³ It is remarkable that the widths become broader again for the smallest value of a , which can be seen in the cases of $MnSO_4$ and $CuSO_4 \cdot H_2O$. In any case, the curves shown in Fig. 1 may have important bearing on the nature of dipolar and exchange interactions of paramagnetic ions.

* Department of Chemistry, Faculty of Science, Ōsaka University, Ōsaka, Japan.

¹ Kumagai, Ōno, Abe, Shōno, Tachimori, Ibamoto, and Shimada, Phys. Rev. **82**, 954 (1947).

² J. H. Van Vleck, Phys. Rev. **74**, 1168 (1948).

³ J. H. Van Vleck and W. G. Penny, Phil. Mag. **17**, 961 (1934).

Erratum: Angular Distribution of Protons from the $D(d, p)T$ Reaction at 10.3-Mev Bombarding Energy

[Phys. Rev. **82**, 782 (1951)]

J. C. ALLRED, D. D. PHILLIPS, AND LOUIS ROSEN
University of California, Los Alamos Scientific Laboratory,
Los Alamos, New Mexico

THE captions of Fig. 1 and Fig. 2 should be interchanged. This applies also to the angle designations on the histograms, i.e., $\theta = 132.5^\circ$ lab for Fig. 2 and $\theta = 12.8^\circ$ for Fig. 1. In addition, these angles should be transposed in the references of the text to the figures.